

J Mater Sci (2007) 42:4745–4752  
DOI 10.1007/s10853-006-0828-7

# Effect of CeO<sub>2</sub> on dielectric, ferroelectric and piezoelectric properties of PMN–PT (67/33) compositions

Benudhar Sahoo · Prasanta Kumar Panda

Received: 7 January 2006 / Accepted: 21 August 2006 / Published online: 19 March 2007  
© Springer Science+Business Media, LLC 2007

**Abstract** Lead magnesium niobate–lead titanate [Pb(Mg<sub>1/3</sub>Nb<sub>2/3</sub>)O<sub>3</sub>–PbTiO<sub>3</sub>] powders doped with different mole % of CeO<sub>2</sub> were prepared by a modified columbite route with compositions corresponding to morphotropic phase boundary (MPB) region. These powders were calcined at 800 °C for 4 h and circular test specimens were prepared by uniaxial pressing. The specimens were sintered at 1150 °C/2 h, poled at 2 kV/mm d.c. voltage and were characterized for dielectric, ferroelectric and piezoelectric properties. It was observed that the piezoelectric and ferroelectric properties initially increase up to 2 mol% of ceria addition and then decrease with increase in ceria concentration. The diffusivity of the dielectric curves increases with increase in ceria concentration. The decrease in Curie temperature was observed from 173 °C corresponding to pure PMN–PT to a temperature of 138 °C for 10 mol% of ceria addition.

## Introduction

Pb(Mg<sub>1/3</sub>Nb<sub>2/3</sub>)O<sub>3</sub>–PbTiO<sub>3</sub> ceramics are known for their high electrostrictive, piezoelectric and dielectric properties [1–4]. It is a very attractive material used for various applications such as multilayer capacitor and electromechanical systems etc. [5–8]. It is a crystalline solid solution of two perovskites. (i) Pb(Mg<sub>1/3</sub>Nb<sub>2/3</sub>)O<sub>3</sub> (PMN), a relaxor ferroelectric with a diffused phase transition and with a

curie temperature ( $T_c$ ) of –15 °C and (ii) PbTiO<sub>3</sub> (PT), a normal ferroelectric with a sharp phase transition and with a  $T_c$  of 490 °C. The addition of PT to PMN shifts the temperature of dielectric maximum to higher temperature [9].

PMN–PT solid solution exhibits a morphotropic phase boundary (MPB) between a rhombohedral phase and a tetragonal phase near compositions of about 30–35 mol% PT [10, 11] where dielectric and piezoelectric constants [4, 12] are very high. Similar to PZT system the properties of PMN–PT are enhanced further by the addition of dopants. Wu et al. [13] studied the La-doped PMN–PT materials and were observed that there is a change of ferroelectric transition from normal to a diffuse one with increase in La content and the piezoelectric coefficient was largely improved with increasing La content. Zhong et al. [14, 15] reported the effect of fixed amount (2 mol%) of rare earth elements such as Sm, Nd, Yb, Ce and also some transition element oxides like WO<sub>3</sub>, etc. on dielectric properties of 0.67PMN–0.33PT composition. They reported that the doping of Sm, Nd and Yb showed a normal ferroelectric behavior but Ce doped samples showed a relaxor like ferroelectric behavior in their dielectric constant versus temperature curve and the dielectric maxima of WO<sub>3</sub> doped sample increased up to 0.5 mol% which then decreased with increase in WO<sub>3</sub> content. Wang and Tang [16] studied the effect of “Ta” on dielectric properties of PMN–PT ceramics and reported that the dielectric constant significantly increases with 10% Ta-doping and exhibited a sharp peak with less frequency dispersion in its dielectric curve.

To our knowledge, there is no literature available on effect of ceria on PMN–PT system although its effect has been studied in other system such as BaTiO<sub>3</sub> [17, 18]. According to Issa et al. [19], the permittivity of BaTiO<sub>3</sub>

B. Sahoo · P. K. Panda (✉)  
Materials Science Division, National Aerospace Laboratories,  
Airport Road, Kodihalli, Bangalore 560 017, India  
e-mail: pkpanda@css.nal.res.in

increases with CeO<sub>2</sub> addition up to 0.5 mol%, and then decreases with increasing CeO<sub>2</sub> concentrations. Similarly, the curie temperature decreases to 92 °C by addition of 0.05–2 mol % of CeO<sub>2</sub>. Park and Song [17] reported that addition of CeO<sub>2</sub> to BaTiO<sub>3</sub> decreases the ferroelectric transition temperature ( $T_c$ ) of cubic–tetragonal forms. In this study, an attempt has been made to study the effect of CeO<sub>2</sub> on the dielectric, ferroelectric and piezoelectric properties of PMN–PT materials.

### Experimental procedure

Reagent grade basic MgCO<sub>3</sub> (Nice chemicals, 99.5%), fine particle sized Nb<sub>2</sub>O<sub>5</sub> powder (SD fine chemicals, 99.5%), lead acetate (Loba chemicals, 99.5%), TiO<sub>2</sub> powder (SD fine chemicals, 99.5%) and CeO<sub>2</sub> powders (IRE, 99.99%) were used as precursors. The concentration of MgO in basic MgCO<sub>3</sub> was estimated gravimetrically. A modified columbite root was adopted for the preparation of ceria doped PMN–PT materials. Excess 3% MgO was added to minimize the pyrochlore phase formation [1, 18, 20]. In the first stage required amount of basic MgCO<sub>3</sub> was slowly dissolved in an appropriate amount of 10% oxalic acid solution at room temperature and low pH was maintained to keep the oxalates in the solution form. Nb<sub>2</sub>O<sub>5</sub> powder was then dispersed in the above solution. The liquid portion was evaporated slowly by gentle heating leaving well-dispersed Nb<sub>2</sub>O<sub>5</sub> powder uniformly coated with magnesium oxalate. The powder was calcined at 1,050 °C for 6 h [21] for columbite phase formation and the phase purity was confirmed by XRD.

In the second stage, TiO<sub>2</sub> and CeO<sub>2</sub> powders were dispersed in calculated amount of Pb(CH<sub>3</sub>COO)<sub>2</sub> solution. Ten percent oxalic acid solution was slowly added with constant stirring in order to precipitate lead oxalate. The precipitate was dried to obtain a homogeneous mixture of lead oxalate, TiO<sub>2</sub> and CeO<sub>2</sub> powder. This powder was thoroughly mixed with columbite powder obtained in the first stage and were calcined at 850 °C for 4 h for PMN–PT phase formation. This calcined powder was milled for 4 h for deagglomeration and with 2% PVA binder, the powders were uniaxially pressed into discs of 2–2.5 mm thickness and were sintered at 1150 °C for 2 h in a closed lead rich atmosphere. The phases present in the calcined powders of columbite and PMN–PT were identified by XRD (M/s. Phillips, Holland) with  $2\theta$  from 20° to 60° at a scanning rate of 2°/min. The morphology of the sintered body was observed by scanning electron microscopy (SEM). The density of the sintered samples was measured by Archimedes principle. For electrical measurements, the sintered compacts were ground and polished to have parallel surfaces, ultrasonically cleaned and electroded with silver

paste. After air-drying, the specimens were cured at 600 °C for ½ h. The dielectric and loss factor measurements were carried out on an automated LCZ meter (1061, Zentech) with variation of temperature as well as frequency. The Curie temperature ( $T_c$ ) of the samples was obtained from the dielectric measurements at the point of maxima. For measurement of piezoelectric properties specimens were poled in silicon oil under an electric field of 2 kV/mm and the values were measured by a piezometer (Model PM-35, M/s. Take control, UK). The remnant polarization ( $P_r$ ), saturation polarization ( $P_s$ ) and coercive field ( $E_c$ ) of the samples were recorded at 50 Hz with an ac field of 25 kV/cm by a modified Sawyer-Tower circuit (M/s Digital systems, Model HLT-2, Mumbai).

### Results and discussion

#### X-ray diffraction

From Fig. 1 it is observed that columbite powder with 3% excess MgO has a single perovskite phase. This is in good agreement with the observations made by previous workers [1, 18, 20]. X-ray diffraction patterns of calcined PMN–PT powders were shown in Fig. 2. While pyrochlore phase was absent in samples with small amount of ceria (up to 2 mol%), it was found present in the samples with higher concentration of ceria. The ratio of relative intensity of the (222) plane of pyrochlore phase ( $I_{PYRO}$ ) to the (110) plane of perovskite PMN–PT phase ( $I_{PEROV}$ ) were used to measure the volume percent of pyrochlore as per Eq. 1:

$$\% \text{ Pyrochlore} = \frac{(I_{PYRO})}{(I_{PEROV}) + (I_{PYRO})} \times 100 \quad (1)$$

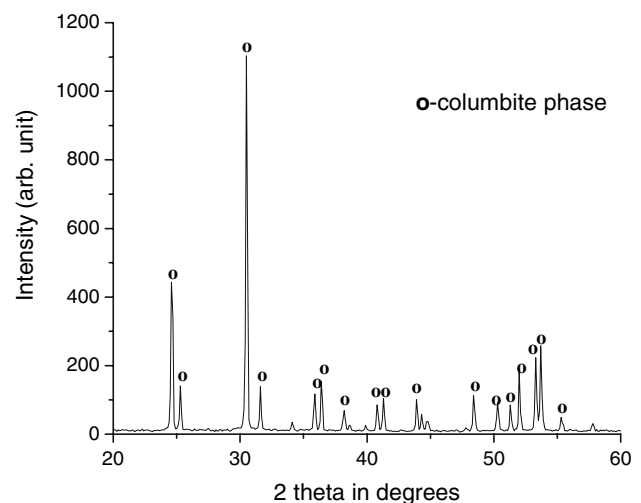
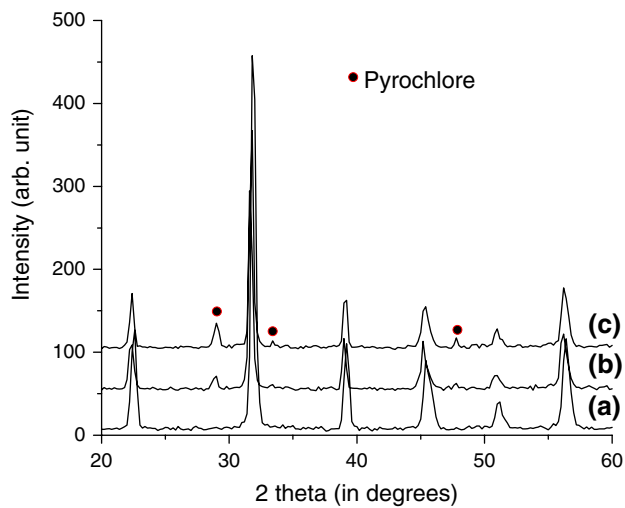


Fig. 1 XRD of columbite powder

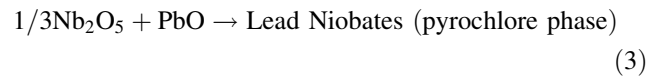
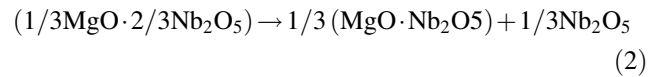


**Fig. 2** XRD pattern of (a) 2, (b) 5, and (c) 10 mol% of ceria doped PMN-PT powders

Based on the above, pyrochlore phase was measured to be 15% and 30% for samples with 5 and 10 mole% of ceria, respectively. This is similar to the observation made by earlier workers on higher mole % of La modified PMN powders [22]. The explanation for the excess pyrochlore phase formation in case of higher ceria doped (5–10 mol%) PMN-PT is as follows.

The addition of ceria dopants is expected to replace “A” site  $Pb^{2+}$  by  $Ce^{3+}$  causing lead vacancy. This is similar to the study made by Chen et al. [23] on  $La^{3+}$  doped PMN. Since, lead vacancies are not favorable defect species in this system; therefore, magnesium niobate is

precipitated to restore the equi-molar ratio of A and B in the  $A(B'B'')O_3$  perovskite PMN-PT structure. The precipitation of magnesium niobate is associated with release of  $Nb_2O_5$  due to its excess ( $MgO:Nb_2O_5 = 1:2$ ) in PMN structure. This could be explained as follows:

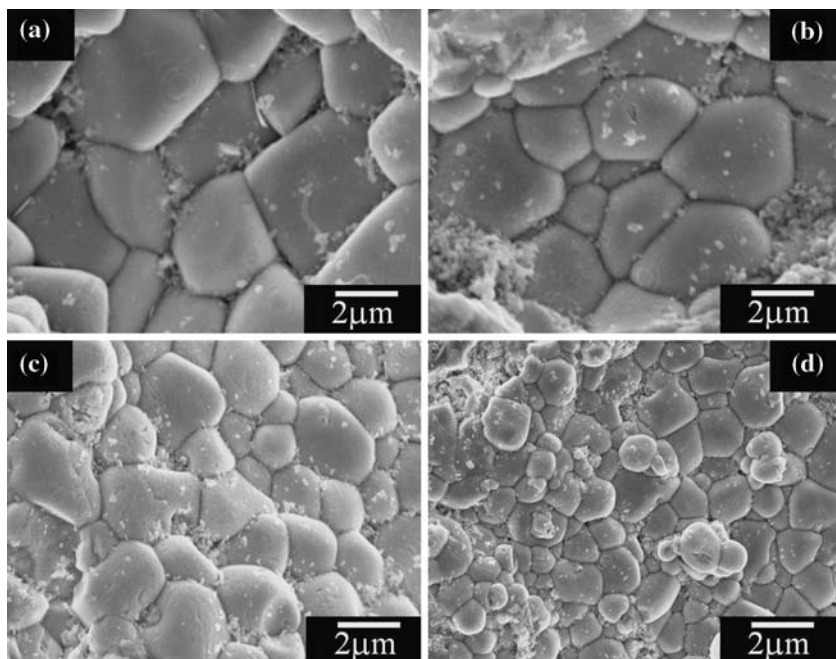


Therefore, the above reactions suggest that higher ceria addition creates higher lead vacancies, which increases the pyrochlore formation.

#### Microstructure and density

Typical SEM micrographs of the etched surfaces of the sintered PMN-PT samples are shown in Fig. 3a–d. The micrographs suggest that materials comprise of polycrystalline microstructure and the percentage of doping affect the microstructure. The sample shows well-developed grains and it is observed that the grain size decreases as the ceria content increases. The size of the grains decreases with the increase in Ce concentration and the micrographs indicate the presence of grains with 5–7  $\mu m$  for 2 mol% of ceria. The PMN-PT sample with 2 mol% of ceria shows a fairly uniform distribution of grain size through out the surface but it becomes non-uniform as the ceria

**Fig. 3** SEM pictures of chemically etched (a) 0, (b) 2, (c) 5 and (d) 10 mol% ceria doped PMN-PT samples



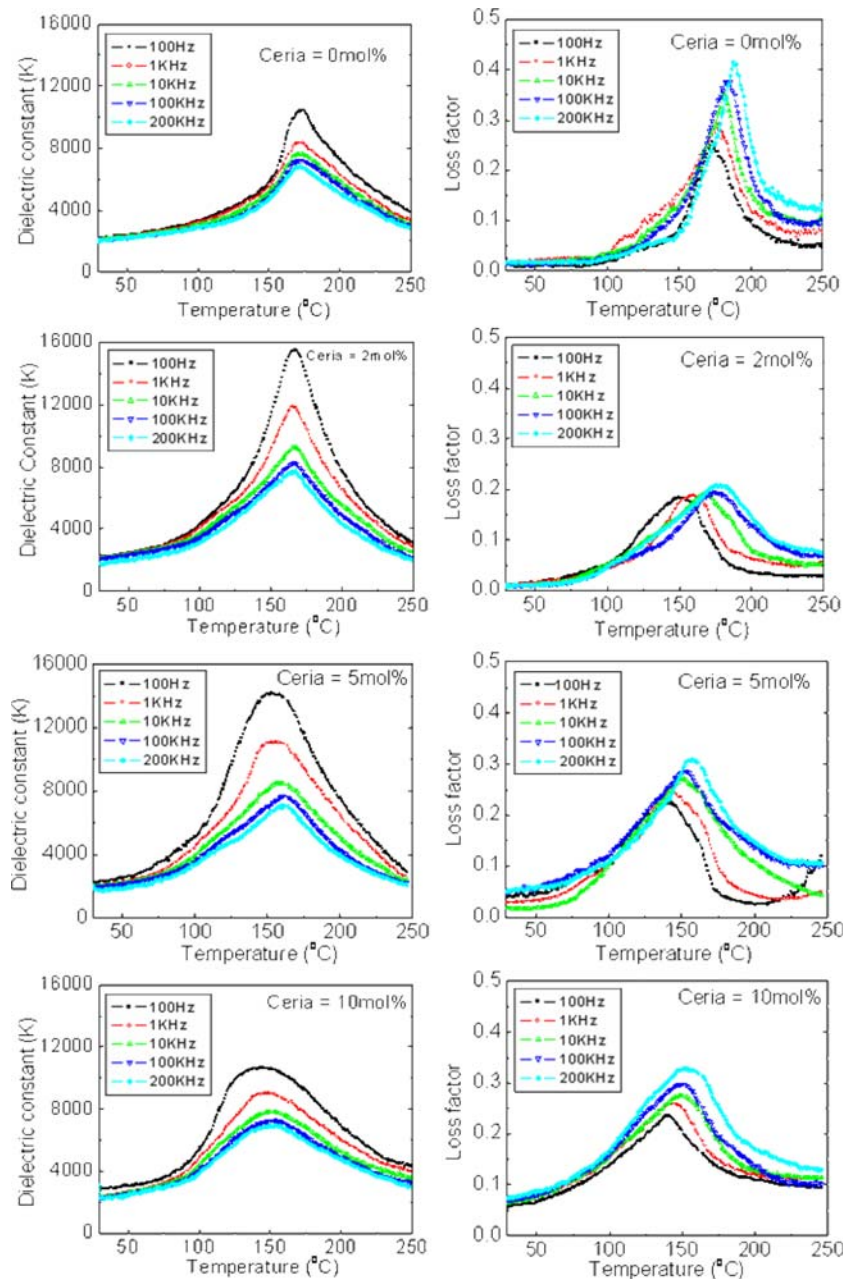
concentration increases. For most of the ferroelectric materials, ferroelectric properties, such as dielectric constant, saturated polarization, remnant polarization and coercive field, are all dependent on grain size of the materials [24]. Damjanovic and Demartin [25] and Randall et al. [26] reported on  $\text{BaTiO}_3$  and  $\text{Pb}(\text{Zr}_{1-x}\text{Ti}_x)\text{O}_3$  systems, respectively, that the number of domain variants will increase with the increase of the grain size. This is because increase in grain size reduces the volume fraction of grain boundaries. As a result, the coupling effect between the grain boundaries and the domain wall (which makes domain reorientation more difficult and severely constrains the domain wall motion) will decrease. Thus the domain

wall mobility will increase, leading to an increase in dielectric constant, with grain size. The densities of the sintered samples was measured by Archimedes's principle and are 7.62, 7.85, 7.76 and 7.71, respectively, for 0, 2, 5 and 10 mol% of ceria doped PMN–PT samples.

#### Dielectric properties

Figure 4 shows the variation of dielectric constant ( $K$ ) and loss factor with temperature at different frequencies (0.1 KHz–200 KHz) for 0, 2, 5 and 10 mol% of ceria doped PMN–PT samples as representative figures. In case of pure PMN–PT, there is a gradual increase in dielectric

**Fig. 4** Temperature variation of dielectric constant ( $K$ ) and loss factor with different mol% of ceria at different frequency



constant up to 173 °C and then decreased further with the increase in temperature measured up to 250 °C. With the increase in frequency, the maxima of the dielectric constant peak were found decreased and the loss factor increased. The increase in “*K*” value up to transition temperature is in the expected lines and could be due to the dominance of interfacial polarization over dipolar polarization [27].

It is also observed from the Fig. 5 that the dielectric constant (*K*) of all the samples increases slowly as the temperature increases to a certain value. At high temperature the observed *K* value increases much faster with temperature exhibiting a maximum value (*K<sub>m</sub>*) at transition temperature (*T<sub>m</sub>*) after which it starts decreasing. The magnitudes of *K* increases up to 2 mol% of ceria and then decreases as ceria concentration increases. This could be explained based on the grain size observed from SEM studies on polished sintered PMN–PT specimens (Fig. 2). From the figure, it is clear that the grain size decreases with the increase in ceria concentration. The higher grain size at lower concentration is attributed to the minimum pyrochlore level, which increases with the ceria content similar to the observation made by XRD studied. The higher dielectric constant for the samples containing less ceria is due to the minimum pyrochlore phase. A reverse trend was observed in case of tanδ, which is obvious.

The values of *T<sub>m</sub>* of the samples were noted from the dielectric versus temperature profile. It was observed from the Fig. 6 that *T<sub>m</sub>* is about 173 °C for undoped composition and gradually decreased to 138 °C for 10 mol% of ceria doping. This observation is in the expected line since addition of dopants decreases *T<sub>m</sub>*.

It can be also observed the mode of transition for the ceria substituted samples look to be diffused at higher concentration (>2 mol%). The above feature can be understood qualitatively by analyzing the data using the

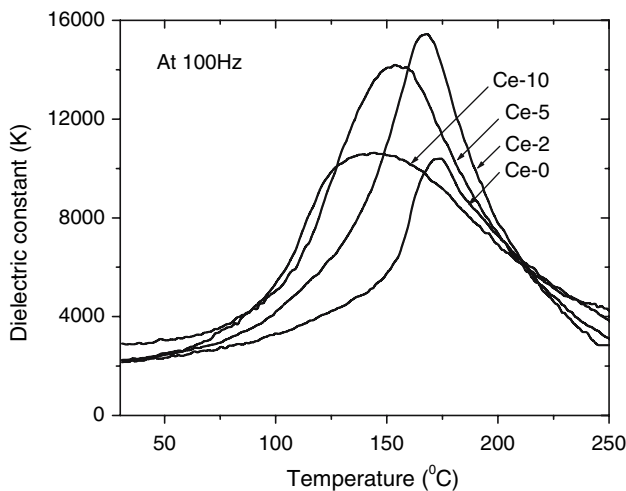


Fig. 5 Change in dielectric constant (*K*) with different mol% of ceria at 100 Hz frequency

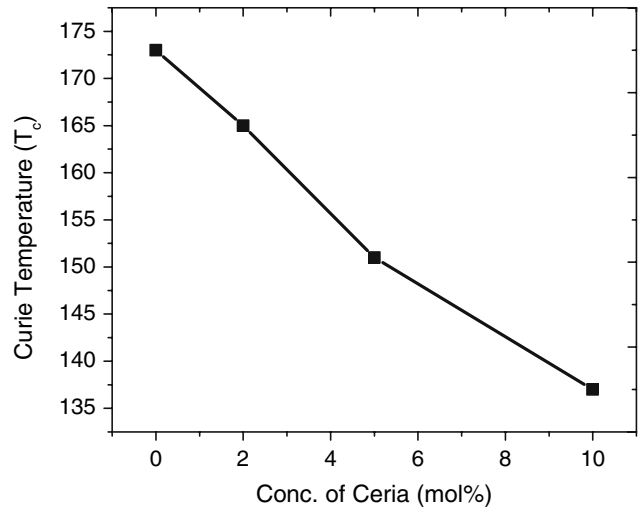


Fig. 6 Change of Curie temperature with different mol% of ceria at 100 Hz frequency

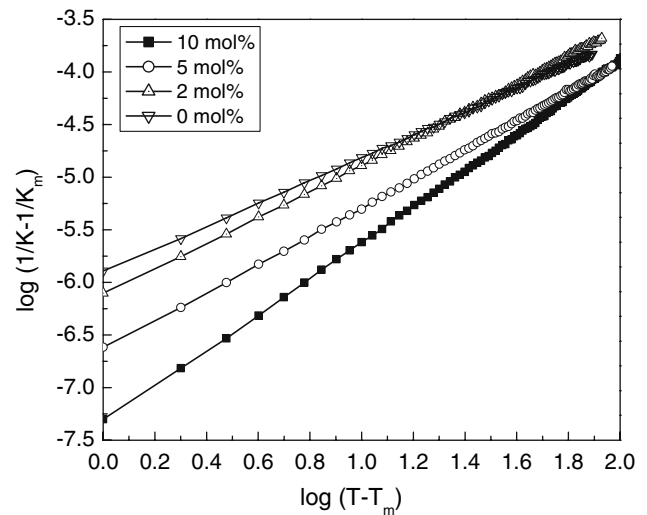


Fig. 7 Plot of  $\log (1/K - 1/K_m)$  vs.  $\log (T - T_m)$  for ceria doped PMN–PT samples at 100 Hz

empirical formula proposed by Uchino and Nomura [28] as:

$$1/K = 1/K_m + (T - T_m)^2/C \tag{4}$$

Table 1 Dielectric parameters at 100 Hz for ceria doped PMN–PT samples

% of Ceria	<i>K<sub>max</sub></i>	<i>T<sub>max</sub></i> (°C)	$\gamma$
0	10,405	173	1.08
2	15,454	165	1.25
5	14,212	153	1.40
10	10,640	138	1.65



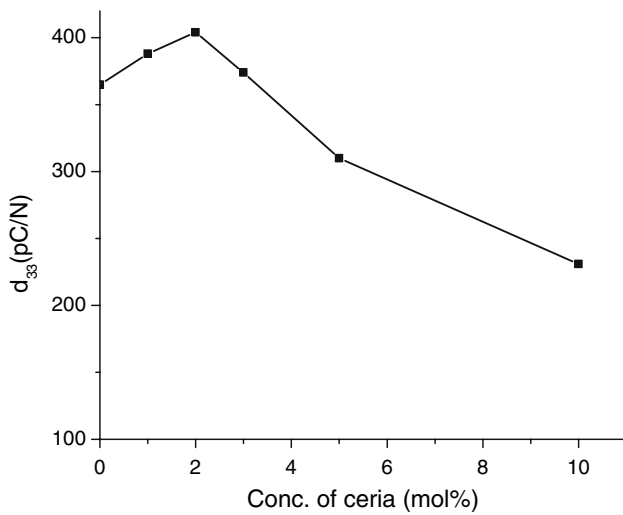


**Fig. 8** Change in  $d_{33}$  with different mol% of ceria

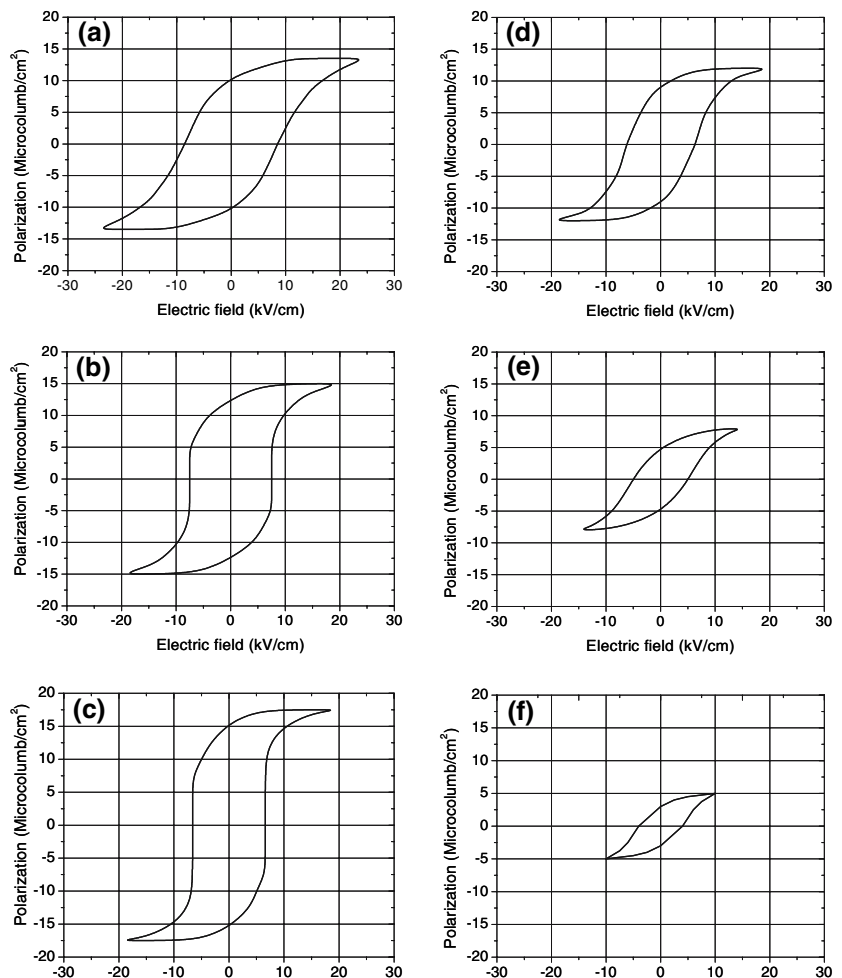
where,  $\gamma$  is the diffuseness exponent and varies between 1 and 2 depending on the nature of the phase transition. For  $\gamma = 1$ , Eq. 1 reduces to Curie–Weiss law and for  $\gamma = 2$ , it

becomes quadratic law. The value of  $\gamma$  can be determined from the slope the plot of  $\log(1/K - 1/K_m)$  versus  $\log(T - T_m)$ , which is shown in Fig. 7 for different ceria amount at 100 Hz. The values of  $\gamma$  are given in Table 1. It is seen that the values are very close to 1 up to 2 mol%  $\text{CeO}_2$  indicating that the compounds obey Curie–Weiss law above the transition temperature. The values are comparatively high for higher concentration of ceria (reaches 1.65 for 10 mol%), which indicates the increase in the diffuseness of the system. This diffuseness could be due to higher compositional fluctuations and structural disordering associated with higher dopant level.

### Piezoelectric properties

The change in piezoelectric charge coefficient ( $d_{33}$ ) of the ceria doped PMN–PT samples were shown in Fig. 8. It is observed that, the  $d_{33}$  value initially increases up to 2 mol% and then decreases with increase in ceria concentration. This behavior is attributed to (i) the soft nature due to addition of  $\text{Ce}^{3+}$  in place of  $\text{Pb}^{2+}$  and also due to (ii)

**Fig. 9** Hysteresis loops of PMN–PT compositions doped with (a) 0, (b) 1, (c) 2, (d) 3, (e) 5, (f) 10 mol% of ceria



formation of pyrochlore phase which is precipitated near the grain boundaries, therefore, hinders the domain wall movement. This is similar to that reported by Zhong et al. for  $\text{WO}_3$  doped PMN–PT [15]. In addition, the third factor could be the decrease in grain size as observed from SEM pictures might contribute in lowering the piezo-properties by hindering the domain wall movement.

#### Ferroelectric properties (hysteresis loop)

The typical hysteresis loop of ceria doped PMN–PT samples at room temperature were shown in Fig. 9. A high electric field (20–25 kV/cm) was required to obtain saturation polarization. From the above figure, it is clearly evident that the shape of  $P$ – $E$  loops varies greatly with the ceramic compositions. The hysteresis loop of 2 mol % ceria has a typical “square” form. This is a typical characteristic of a phase that contains long-range interaction between dipoles in the ferroelectric micro-domain state. The saturation polarization ( $P_s$ ), remnant polarization ( $P_r$ ) and coercive field ( $E_c$ ) were determined from the hysteresis loop. From Fig. 10, it is observed that, the value of polarization increases up to 2 mol% of ceria and then decreased with increase in doped ion concentration. The coercive field gradually decreases with increase in ceria concentration. This phenomenon can be interpreted in terms of polarization mechanism. It is observed from the Fig. 6 that the diffusivity of the curves gradually increases with ceria concentration, which indicates the increase of relaxor behavior in the samples. Due to this the reorientation of microdomains cannot contribute much to  $E_c$  during the polarization, and the lower values may be attributed to electrostriction, induced mainly by dipolar and ionic polarization [29].

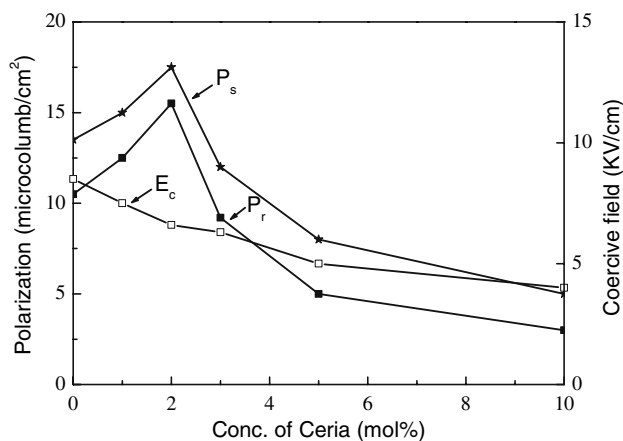


**Fig. 10** Plot of  $P_s$  &  $P_r$  and  $E_c$  at different mol% of ceria

## Conclusions

Ceria doped PMN–PT samples were prepared by a modified columbite route and were characterized for ferroelectric, piezoelectric and dielectric properties. The dopant enhanced the piezoelectric and ferroelectric properties up to 2 mol% by facilitating easier domain wall movement due to the soft behavior induced by  $\text{Ce}^{3+}$  in place of  $\text{Pb}^{2+}$ . Thereafter, the above properties further decreases with increase in dopant concentration due to the formation of pyrochlore phase, precipitation of excess dopant near the grain boundaries hindering the domain wall movement. The nature of ferroelectric transition from normal to diffused type was observed by the incorporation of higher amounts of ceria (>2 mol%). The transition temperature was 173 °C for pure PMN–PT and then gradually reduced to 138 °C with the increase of ceria content up to 10 mol%.

**Acknowledgements** The authors are very grateful to Dr. S. Usha Devi for XRD patterns, Mr. M.A. Venkatswami and Mrs. Kalavati for SEM. The authors also gratefully acknowledge Head, Materials Science Division and Director, NAL for providing necessary encouragement during the course of this study. The authors would like to thank Prof. V. Subramanian and D. Rout, Department of Physics, IIT Madras for their help in measurement of dielectric constant of the samples. Mr. Benudhar Sahoo also thanks CSIR, New Delhi for the research fellowship.

## References

- Swartz SL, Shrout TR, Schulze WA, Cross LE (1984) J Am Ceram Soc 67:311
- Ouchi H, Nagano K, Hayakawa S (1965) J Am Ceram Soc 48:630
- Cross LE, Jang SJ, Newnham RE, Nomura S, Uchino K (1980) Ferroelectrics 23:187
- Choi SW, Shrout TR, Jang SJ, Bhalla AS (1989) Mater Lett 8:253
- Markgra SA, Bhalla AS (1996) Mater Lett 28:221
- Uchino K (1986) Am Ceram Soc Bull 65:647
- Cross LE (1996) Mater Chem Phys 43:108
- Colla EV, Gupta SM (1999) J Appl Phys 85:362
- Choi SW, Shrout TR, Jang SJ, Bhalla AS (1989) Ferroelectrics 100:29
- Eugene VC, Yushin NK, Viehland D (1998) J Appl Phys 83:3298
- Gene HH (1999) J Am Ceram Soc 82:797
- Ho JC, Liu KS, Lin IN (1993) J Mater Sci 28:4497
- Wu TB, Shyu MJ, Chung CC, Lee HY (1995) J Am Ceram Soc 78(8):2168
- Zhong N, Xiang P, Sun D, Dong X (2005) Mater Sci Eng B 116:140
- Zhong N, Dong X, Sun D, Xiang P, Du H (2004) Mater Res Bull 39:175
- Wang JT, Tang F (2002) Mater Chem Phys 75:86
- Park Y, Song SA (1995) J Mater Sci Mater Electron 6:380
- Lejeune M, Boilot JP (1986) Am Ceram Soc Bull 64:679
- Issa MAA, Molokhia NM, Dughaiash ZH (1983) J Phys D: Appl Phys 16:1109
- Yan MF, Ling HC, Rhodes WW (1989) J Mater Res 4:930
- Panda PK, Sahoo B (2005) Mater Chem Phys 93:231

22. Gupta SM, Viehland D (1997) *J Am Ceram Soc* 80:477
23. Chen J, Helen M, Harmer MP (1989) *J Am Ceram Soc* 72:593
24. Rout D, Subramanian V, Hariharan K, Sivasubramanian V (2005) *Mater Sci Eng B* 123:107
25. Damjanovic D, Demartin M (1996) *Appl Phys Lett* 68:3046
26. Randal CA, Kim N, Kucera JP, Cao W, Shrout TR (1998) *J Am Ceram Soc* 81:677
27. Hench LL, West JK (1990) *Principles of electronic ceramics*. Wiley, New York
28. Uchino K, Nomura S (1982) *Ferroelectrics Lett* 44:55
29. Sundar V, Newnham RE (1992) *Ferroelectrics* 135:431